Chemical Geology 627 (2023) 121455

Contents lists available at ScienceDirect

Chemical Geology

journal homepage: www.elsevier.com/locate/chemgeo

Boron isotope fractionation between $B(OH)_3$ and $B(OH)_4^-$ in aqueous solution: A theoretical investigation beyond the harmonic and Born−Oppenheimer approximations

Xinya Yin [a,1], Feixiang Liu [b,1], Qi Liu [b,*], Yining Zhang [b], Caihong Gao [b], Siting Zhang [c,d], Moira K. Ridley [e], Yun Liu [b,d,f]

[a] School of Civil Engineering and Architecture, Guizhou Minzu University, Guiyang 550025, China
[b] State Key Laboratory of Ore Deposit Geochemistry, Institute of Geochemistry, Chinese Academy of Sciences, Guiyang 550081, China
[c] Center for Lunar and Planetary Science and State Key Laboratory of Ore Deposit Geochemistry, Institute of Geochemistry, Chinese Academy of Sciences, Guiyang 550081, China
[d] CAS Center for Excellence in Comparative Planetology, Hefei 230026, China
[e] Department of Geosciences, Texas Tech University, Lubbock, TX 79409, United States
[f] International Center for Planetary Science, College of Earth Sciences, Chengdu University of Technology, Chengdu 610059, China

ARTICLE INFO

Editor: Michael E. Boettcher

Keywords:
Boron isotope fractionation
Aqueous solution
Solvation effect
Anharmonicity
Diagonal born−Oppenheimer correction

ABSTRACT

Boron isotope fractionation between boric acid and borate ion in aqueous solution (hereafter, α_{3-4}) is a key coefficient for reconstructing paleo-pH and paleo-pCO_2 records, and a valuable parameter for understanding boron isotope geochemistry related to mineral-water interactions. Although boron isotopes have wide geologic application, the effect of temperature and ion pairing on boron isotope fractionation is poorly described. Moreover, conventional density functional theory (DFT) calculations do not provide an accurate estimate of the boron isotope fractionation factor. Here, we provide a new strategy to accurately calculate α_{3-4} values in aqueous solution by evaluating harmonic frequencies, higher-order energy terms, and solvation effects. Using benchmark coupled cluster (CCSD(T)) calculations, our 25 °C results for α_{3-4} ranges from 1.0259 to 1.0275, which is in good agreement with recent experimental data. Solvation effects reduced the α_{3-4} value by ~6‰, while high-order corrections raised the α_{3-4} value by ~2‰. Our calculations evaluating the effect of aqueous ion pairs suggest that the α_{3-4} values in seawater and pure water should be almost identical. Our results provide a reasonable estimation of the partition function ratios of dissolved boron species, which will benefit studies of boron isotope fractionation in aqueous environments.

1. Introduction

Boron species exist mainly as boric acid ($B(OH)_3$) and borate ion ($B(OH)_4^-$) in aqueous solution, where $B(OH)_4^-$ is the hydrolysis product of $B(OH)_3$. The proportion of the two boron species is controlled by pH (Hershey et al., 1986). In seawater, total boron concentration [B_T] is ~432.6 μmol/kg, thus the formation of polyborate species is negligible (Ingri et al., 1957; Lee et al., 2010). The residence time of boron in seawater is ~10–20 million years, much greater than the mixing time of the oceans (Lemarchand et al., 2002; Simon et al., 2006). Thus, the boron isotope composition of $B(OH)_4^-$ in marine carbonates (assuming co-precipitated), can serve as a proxy for oceanic pH and atmospheric CO_2 (Vengosh et al., 1991; Hemming and Hanson, 1992; Spivack et al., 1993; Hemming et al., 1995; Sanyal et al., 1996).

To use boron isotopes as a paleo-pH proxy, it is necessary to accurately determine boron isotope fractionation between $B(OH)_3$ and $B(OH)_4^-$, and the fractionation temperature dependence (Pagani et al., 2005; Liu and Tossell, 2005; Klochko et al., 2006; Hönisch et al., 2019). As the α_{3-4} value is difficult to measure, early studies using the boron isotope proxy to reconstruct oceanic pH and atmospheric pCO_2 adopted the theoretical value of α_{3-4} = 1.0194, predicted by Kakihana et al. (1977) (e.g., Sanyal et al., 1995; Palmer et al., 1998; Pearson and Palmer, 1999; Pearson and Palmer, 2000; Palmer and Pearson, 2003; Hönisch and Hemming, 2005). However, subsequent quantum chemical

* Corresponding author.
E-mail address: liuqi@mail.gyig.ac.cn (Q. Liu).
[1] These authors contributed equally to this article and should be regarded as co-first authors.

https://doi.org/10.1016/j.chemgeo.2023.121455
Received 29 December 2022; Received in revised form 18 March 2023; Accepted 29 March 2023
Available online 4 April 2023

calculations showed that the prediction of Kakihana et al. (1977) might underestimate the $\alpha_{3\text{-}4}$ value (Oi, 2000a, 2000b; Oi and Yanase, 2001; Liu and Tossell, 2005; Zeebe, 2005). Oi (2000b) used frequency-scaled HF (Hartree-Fock), MP2 (second-order Møller-Plesset perturbation theory) and DFT (density functional theory) methods to calculate the $\alpha_{3\text{-}4}$ value between gaseous boron species, and concluded that the true $\alpha_{3\text{-}4}$ value at 25 °C would be between 1.019 and 1.033. Although Oi (2000b) did not offer a definitive $\alpha_{3\text{-}4}$ value for the gas phase, Oi and Yanase (2001) suggested using the HF/6-31G(d) theory level for further calculations of boron isotope effects in the liquid phase. Liu and Tossell (2005) then used the frequency-scaled HF/6-31G(d) method to calculate the $\alpha_{3\text{-}4}$ values in aqueous solution and suggested an $\alpha_{3\text{-}4}$ value of ~1.027 can be used for the boron isotope pH-proxy. However, the $\alpha_{3\text{-}4}$ values calculated by Zeebe (2005) using force fields and quantum chemical models varied from ~1.020 to ~1.050 at 300 K, depending on the choice of frequency and method. Zeebe (2005) results challenged the accuracy of theoretical predictions. In contrast to quantum chemical calculations, the vibrational spectroscopic data of Sanchez-Valle et al. (2005) reported an even smaller $\alpha_{3\text{-}4}$ value of 1.0176 at 300 K. Consequently, experimental measurements were expected to provide constraints on the $\alpha_{3\text{-}4}$ value (Zeebe, 2005).

With analytical advances in spectrophotometric measurements, it became feasible to determine $\alpha_{3\text{-}4}$ in aqueous solution by measuring pH differences between pure ^{10}B or ^{11}B buffered solutions (i.e., $\alpha_{3\text{-}4}$ = 1.0285 ± 0.0016 at 25 °C in KCl solution, Byrne et al., 2006). Klochko et al. (2006) employed spectrophotometric pH measurements to determine $\alpha_{3\text{-}4}$ values in several solutions, and obtained $\alpha_{3\text{-}4}$ values of 1.0308 ± 0.0023 (25 °C) and 1.0289 ± 0.0048 (40 °C) in pure water, and 1.0272 ± 0.0006 (25 °C) and 1.0269 ± 0.0027 (40 °C) in artificial seawater. Recently, Nir et al. (2015) developed an alternative method to determine $\alpha_{3\text{-}4}$ by isolating $B(OH)_3$ through a reverse osmosis membrane under controlled pH conditions, and calculated the $\alpha_{3\text{-}4}$ value in seawater-like solutions as 1.026 ± 0.001 at 25 °C from mass balance. The $\alpha_{3\text{-}4}$ values for seawater obtained by Klochko et al. (2006) and Nir et al. (2015) are in good agreement with the theoretical prediction of Liu and Tossell (2005), confirming that the boron isotope fractionation in aqueous solution is larger than the original prediction of Kakihana et al. (1977). However, the prediction of Liu and Tossell (2005) indicated that the $\alpha_{3\text{-}4}$ values decrease as temperature increases and are very similar in pure water and seawater, while the $\alpha_{3\text{-}4}$ values measured by Klochko et al. (2006) show no temperature dependence within experimental uncertainties and show a statistical difference between pure water and seawater. Pure water and seawater differ significantly in terms of ionic strength and ion species. Therefore, difference between measured $\alpha_{3\text{-}4}$ values in pure water and seawater suggest that ion pairing of dissolved boron species may play an important role in boron isotope fractionation between $B(OH)_3$ and $B(OH)_4^-$ or during boron incorporation. On the other hand, from thermodynamic principles, isotope fractionation factors should show temperature dependent effects. Experimental uncertainties that masked the temperature dependences of $\alpha_{3\text{-}4}$ in Klochko et al. (2006) may also have affected measured differences in the $\alpha_{3\text{-}4}$ values in pure water and seawater. To improve paleo-pH reconstruction, it is important to better constrain the extent to which $\alpha_{3\text{-}4}$ is sensitive to temperature (Hönisch et al., 2019). Additionally, as boron ion pairs in seawater may influence boron incorporation (e.g., Mavromatis et al., 2021; Henehan et al., 2022), it is worth exploring the effects of temperature and ion pairs on both $\alpha_{3\text{-}4}$ values and partition function ratios of dissolved boron species. The results will improve the reconstruction of paleo-pH, and will be valuable to better understand boron isotope effects related to mineral-water interactions; for example, boron isotope fractionation during carbonate precipitation (Balan et al., 2018) and boron isotope fractionation between minerals and fluids (Sanchez-Valle et al., 2005; Kowalski et al., 2013; Li et al., 2020, 2021, 2022).

From the perspective of theoretical calculations, quantum chemical models can provide accurate physicochemical properties of substances (e.g., Daru et al., 2022) to produce reliable isotope fractionation factors that are comparable to experimental determinations; however, the energy shifts associated with isotope substitutions must be accurately calculated (Liu et al., 2010). The Hartree-Fock (HF) method employed by Liu and Tossell (2005) did not calculate correlation energy (Levine, 2014), which describes how electrons influence each other and is important for improving geometry optimizations and energy calculations. Therefore, the good agreement between the prediction of Liu and Tossell (2005) and the $\alpha_{3\text{-}4}$ values measured at 25 °C is surprising. More robust predictions of isotope fractionation factors were expected from DFT and post-HF methods (Rustad and Bylaska, 2007); however, Rustad et al. (2010) found that both DFT and MP2 methods gave diverse $\alpha_{3\text{-}4}$ values. For example, using DFT functionals, reported $\alpha_{3\text{-}4}$ value at 25 °C in pure water were ~ 1.032–1.035; whereas, values of 1.026–1.028 were extrapolated from MP2 methods. In the pure water calculations of Rustad et al. (2010), the results from DFT were close to the value of Klochko et al. (2006) measured in pure water, but the extrapolated $\alpha_{3\text{-}4}$ values from MP2 matched the value obtained for seawater. The Rustad et al. (2010) study raised the question of which quantum chemical models can provide reliable predictions of isotope fractionation factors in solutions. Although the DFT method has been utilized to predict isotope fractionation factors for many isotopic systems (e.g., Anbar et al., 2005; Méheut et al., 2007; Domagal-Goldman and Kubicki, 2008; Li et al., 2009; Fujii et al., 2014; Blanchard et al., 2015; Gao et al., 2018; Hill et al., 2020; Wang et al., 2020; Li et al., 2021), the method still does not provide convincing calculated $\alpha_{3\text{-}4}$ values (Rustad et al., 2010; Kowalski et al., 2013; Li et al., 2020; Zeebe and Rae, 2020). As the previous studies were based on harmonic approximation and predominantly employed DFT to generate harmonic frequencies, improvement in calculated $\alpha_{3\text{-}4}$ values should result from a thorough evaluation of harmonic frequencies, higher-order corrections, and solvation effects.

In this study, we provide a new strategy for the accurate calculation of isotope fractionation between species in solution, and we calculate $\alpha_{3\text{-}4}$ values beyond the harmonic approximation and Born−Oppenheimer approximation. The contributions of higher-order energy terms, solvation effects, and ion pairing are investigated. Accurate temperature dependences of $\alpha_{3\text{-}4}$ and the partition function ratios of dissolved boron species are presented. We show that boron isotope fractionation between $B(OH)_3$ and $B(OH)_4^-$ in aqueous solution can be calculated with reasonable accuracy from quantum chemical methods without any special adjustments, such as scaling frequencies or extrapolating data.

2. Methods

2.1. Equilibrium isotope fractionation theory

Consider an isotopic exchange reaction in the gas phase:

$$AX^L + BX^H = AX^H + BX^L \quad (1)$$

where AX and BX are two substances containing an element of interest X, with X^L and X^H the light and heavy isotopes of element X, respectively. The standard free energy change for this reaction is

$$\Delta E = E_{AX^H} + E_{BX^L} - E_{AX^L} - E_{BX^H} = \Delta E_{AX} - \Delta E_{BX} \quad (2)$$

where ΔE_{AX} and ΔE_{BX} are the energy shifts due to the isotope substitutions, for example,

$$\Delta E_{AX} = E_{AX^H} - E_{AX^L} \quad (3)$$

When the reaction reaches equilibrium at temperature T, the relationship between the equilibrium constant K_{eq} and the relative free energies can be obtained as follows:

$$K_{eq} = exp\left(\frac{-\Delta E}{k_B T}\right) = exp\left(\frac{-\Delta E_{AX}}{k_B T}\right) \Big/ exp\left(\frac{-\Delta E_{BX}}{k_B T}\right) \quad (4)$$

where k_B is the Boltzmann constant. The energy shifts due to isotope substitutions for substances such as AX can be given by

$$\Delta E_{AX} = \Delta E^0_{AX} + \Delta E^{Corr}_{AX} \quad (5)$$

where ΔE^0 is the sum of energy shifts due to an isotope substitution in the rigid-rotor-harmonic-oscillator (RRHO) approximation and the Born−Oppenheimer (BO) approximation (i.e., the energy shifts from translational, rotational, and vibrational energies), and ΔE^{Corr} is the sum of corrections from energy shifts beyond the RRHO and BO approximations. For single isotope substitution, the relationship between the equilibrium isotope fractionation factor α and the equilibrium constant K_{eq} can be expressed as

$$\alpha_{AX-BX} = \frac{s_{AX^H}/s_{AX^L}}{s_{BX^H}/s_{BX^L}} K_{eq} \quad (6)$$

where s is the symmetry number of the isotopologue (Bigeleisen and Mayer, 1947; Schauble, 2004; Liu et al., 2010). From Eqs. (4), (5), and (6), the equilibrium isotope fractionation factor α between AX and BX can be written as

$$\alpha_{AX-BX} = \alpha^0_{AX-BX} \cdot K^{Corr}_{AX-BX} \quad (7)$$

where

$$\alpha^0_{AX-BX} = \frac{\beta(AX^H/AX^L)}{\beta(BX^H/BX^L)} \quad (8)$$

is the Bigeleisen-Mayer equation, and K^{Corr} is the correction term (Bigeleisen, 1996). The β factor (also known as the Reduced Partition Function Ratio, RPFR) of an isotopologue pair (e.g., AX^H/AX^L) is defined as

$$\beta(AX^H/AX^L) = \prod_i \frac{u_i(AX^H)exp[-u_i(AX^H)/2]\{1-exp[-u_i(AX^L)]\}}{u_i(AX^L)exp[-u_i(AX^L)/2]\{1-exp[-u_i(AX^H)]\}} \quad (9)$$

where $u_i = hc\omega_i/k_BT$, h is the Planck constant, c is the speed of light in vacuum, ω_i is the harmonic frequency of normal mode i in cm^{-1}, and T is the temperature in Kelvin (Bigeleisen and Mayer, 1947; Urey, 1947). The correction term K^{Corr} can be obtained by multiplying individual higher-order correction terms, i.e.,

$$K^{Corr}_{AX-BX} = K^{anh}_{AX-BX} \cdot K^{BOELE}_{AX-BX} \cdot K^{hf}_{AX-BX} \cdot K^{fs}_{AX-BX} \cdot \cdots \quad (10)$$

where K^{anh} is the anharmonic vibration correction, K^{BOELE} is the correction to the BO approximation, K^{hf} is the correction for the nuclear spin effect, and K^{fs} is the correction for the nuclear field shift effect (Bigeleisen, 1996).

If the isotopic exchange reaction reaches equilibrium in solution, Eq. (5) then becomes

$$\Delta E_{AX} = \Delta E^0_{AX} + \Delta E^{Corr}_{AX} + \Delta E^{solv}_{AX} \quad (11)$$

where ΔE^{solv} is the sum of energy shifts associated with the solvation effect (Chen et al., 2009; Grimme, 2012). Therefore, the equilibrium isotope fractionation factor α between AX and BX in the liquid phase can be expressed as

$$\alpha_{AX-BX} = \alpha^0_{AX-BX} \cdot K^{Corr}_{AX-BX} \cdot K^{solv}_{AX-BX} \quad (12)$$

and K^{solv} can be obtained from the ratio of α^0 values in the liquid and gas phases, i.e.,

$$K^{solv}_{AX-BX} = (\alpha_{AX-BX}/K^{Corr}_{AX-BX})/\alpha^0_{AX-BX} = \alpha^0_{AX-BX}(l)/\alpha^0_{AX-BX}(g) \quad (13)$$

where l and g refer to the liquid and gas phases, respectively. Eq. (13) is also straightforward in the RRHO and BO approximations. Once accurate α^0, K^{Corr} and K^{solv} values are obtained, the equilibrium isotope fractionation factor between two substances in solution can be determined.

2.2. Computational details

The Gaussian 09 package (Frisch et al., 2013) was used to perform geometry optimizations, single-point energy calculations, harmonic frequency generations and second-order perturbation analyses. The CFOUR package (CFOUR, 2000; Harding et al., 2008a, 2008b) was used to calculate effects beyond BO approximation. To simulate solvation effects, explicit solvent models (so-called "water-droplet" models, Liu and Tossell, 2005; Li et al., 2009) were adopted at the B3LYP/6–311+G(d,p) theory level (Krishnan et al., 1980; McLean and Chandler, 1980; Clark et al., 1983; Frisch et al., 1984; Spitznagel et al., 1987; Lee et al., 1988; Becke, 1993). B3LYP is a hybrid functional in density function theory (DFT), and stands for "Becke, 3-parameter, Lee, Yang, and Parr". 6–311+G(d,p) indicates that the 6–311G basis sets are used for first-row atoms and the McLean-Chandler basis sets are used for second-row atoms by including the diffuse functions (+) and the polarization functions (d,p). Initially, we optimized the $B(OH)_3$, $B(OH)_4^-$, and $B(OH)_4^-$ ion paired species separately in vacuum; we then surrounded the optimized boron species with 6 water molecules and re-optimized the hydrated structure. Thereafter, we added an additional 6 water molecules and re-optimized the structures. Following optimization, we calculated harmonic frequencies. The procedure was repeated, with the incremental addition of 6 water molecules, until the β factors for the boron species converged. The number of water molecules used to simulate the hydration shell of $B(OH)_3$ and $B(OH)_4^-$ was 6, 12, 18, 24, 30, and 36 in sequence. In total, 36 water molecules were used to simulate the hydration shells of $B(OH)_3$ and $B(OH)_4^-$. Considering the complexity of the aqueous environment, we constructed three groups of solvation models and ensured that the layouts of the first 6 water molecules (i.e., part of the primary hydration shell) were different in each model. Because the calculations involve the simulation of weak interactions in solution, B3LYP with a dispersion correction (B3LYP-D3) and a "superfine" integration grid was employed for this study to overcome the inherent deficiency of density functional theory (Grimme, 2011).

For accurate calculations of isotope fractionation factors, corrections of higher-order energy terms need to be considered, especially for the isotope substitutions of light elements (Bron et al., 1973; Richet et al., 1977; Liu et al., 2010). Therefore, seven types of corrections to the Bigeleisen-Mayer equation were evaluated to better calculate $\alpha_{3\text{–}4}$: (1) anharmonic corrections for zero-point energy (AnZPE), (2) anharmonic corrections for vibrational excited states (AnEXC), (3) vibration-rotation coupling corrections for zero-point energy (VrZPE), (4) vibration-rotation coupling corrections for vibrational excited states (VrEXC), (5) quantum mechanical corrections to rotation (QmCorr), (6) centrifugal distortion corrections (CenDist), and (7) diagonal Born−Oppenheimer corrections (DBOC) (Liu et al., 2010; Zhang and Liu, 2018, and the equations and citations within). To calculate these higher-order corrections, we selected the second-order Møller-Plesset perturbation theory method (MP2) (Møller and Plesset, 1934) with the 6–311+G(d,p) basis set (Frisch et al., 1984; Krishnan et al., 1980; McLean and Chandler, 1980) to obtain the effects beyond the harmonic approximation (Liu et al., 2010; Liu and Liu, 2016), and the CCSD/pVTZ theory level (McLean and Chandler, 1980; Purvis and Bartlett, 1982; Woon and Dunning, 1993) for the calculation of DBOC (Zhang and Liu, 2018). Here, the needed higher-order energy terms are obtained only for gaseous $B(OH)_3$ and $B(OH)_4^-$. Comparable effects can be expected in the liquid phase, since the vibrational modes contributing to the calculations of β factors are similar (Balan et al., 2018). According to the results of Rustad et al. (2010), the $\alpha_{3\text{–}4}$ values calculated for the liquid phase are affected by the accuracy of the $\alpha_{3\text{–}4}$ values calculated for the gas phase. To constrain the boron isotope fractionation factor between $B(OH)_3$ and $B(OH)_4^-$ in the gas phase, we used the benchmark results obtained by performing coupled cluster calculations covering the single and double

electron excitations iteratively and the triple electron excitations perturbatively (CCSD(T)), in combination with the basis sets of 6–311+G(d,p) and aug-cc-pVTZ (Riley et al., 2010; Liu et al., 2021), where aug-cc-pVTZ adds diffuse functions (aug-) to the Dunning's correlation consistent basis set cc-pVTZ, that by definition includes polarization functions (Dunning, 1989; Kendall et al., 1992; Woon and Dunning, 1993).

3. Results

3.1. Boron isotope fractionation between $B(OH)_3$ and $B(OH)_4^-$ in the gas phase

Table 1 shows the β_3, β_4 and α^0_{3-4} values calculated for boron isotope exchanges between $B(OH)_3$ and $B(OH)_4^-$ in the gas phase based on the RRHO and BO approximations. Both the β and α values decrease as the temperature increases. The results calculated at the MP2/6–311+G(d,p) and B3LYP/6–311+G(d,p) levels are compared with those calculated at the CCSD(T)/6–311+G(d,p) and CCSD(T)/aug-cc-pVTZ levels. Because CCSD(T) is the "gold standard" of quantum chemistry (Riley et al., 2010), we assumed that the CCSD(T) results gave the most accurate α values; consequently, we selected the CCSD(T) results as our reference values for the harmonic approximation (Liu et al., 2021). The β factors calculated from CCSD(T) methods were well converged. For example, the β_4 factors from CCSD(T)/6–311+G(d,p) and CCSD(T)/aug-cc-pVTZ are almost identical, and the differences between β_3 factors from CCSD(T)/6–311+G(d,p) and CCSD(T)/aug-cc-pVTZ are within 0.002 across the temperature range studied here. The differences between the β factors calculated from the MP2 and the CCSD(T) methods are also small, such that the α^0_{3-4} values calculated at MP2/6–311+G(d,p) level are close to those obtained from the CCSD(T) methods. However, the β and α^0_{3-4} values calculated at the B3LYP/6–311+G(d,p) level show larger discrepancies from the results of CCSD(T) methods, especially the β_4 values. At 25 °C, the α^0_{3-4} values from the CCSD(T) methods range between 1.0305 and 1.0321, which is much lower than the results calculated at the B3LYP/6–311+G(d,p) level. Collectively, our results show that the B3LYP method may overestimate the boron isotope fractionation factor between gaseous $B(OH)_3$ and $B(OH)_4^-$ by ~4–7‰ for the temperature range considered.

3.2. Higher-order corrections

The higher-order corrections to the β_3, β_4 and α_{3-4} factors at 25 °C are listed in Table 2. All corrections were calculated in the gas phase. Because the molecular mass of $B(OH)_3$ or $B(OH)_4^-$ is large, the higher-order corrections related to rotation play an insignificant role in this study. Additionally at room temperature, the higher-order corrections contributed by vibrational excited states are also negligible. Of all corrections, only AnZPE and DBOC contribute significantly to boron isotope substitutions. For example, the contribution of AnZPE reduces the β_3 value by ~5.6‰ at 25 °C. When considering the effects of higher-order corrections, boron isotope fractionation between $B(OH)_3$ and $B(OH)_4^-$ at room temperature should rise by 1.8‰. Therefore, it is necessary to consider the contributions of AnZPE and DBOC in this study.

3.3. Explicit solvent models

To estimate the improvement of utilizing the DFT-D3 method, the results of the B3LYP methods with and without the D3 correction were compared for the explicit solvent models. Table 3 shows the average B—O bond lengths of $B(OH)_3$ and $B(OH)_4^-$ in our solvation models. To better describe the effects of weak interactions, B3LYP-D3(BJ)/6–311+G(d,p) was used, where the -D3(BJ) means a Landon-dispersion correction (D3, Grimme, 2011) employing a rational damping function proposed by Becke and Johnson (2005) (BJ). When n is equal to 0, the results represent the calculations performed in the gas phase. The average B—O bond length of $B(OH)_3$ in aqueous solution increases slightly in length relative to the gas phase, while the B—O bond length of $B(OH)_4^-$ decreases significantly because of the negative charge. The configurations of $B(OH)_3$ and $B(OH)_4^-$ with a hydration shell of 36 water molecules are shown in Fig. 1. A hydration shell of 36 water molecules represents at least 2 layers of water molecules. The inner-hydration layer, which is the most importance for calculating the solvation effects on α_{3-4} values, of the $B(OH)_3$ clusters contain 7 or 8 water molecules, and the $B(OH)_4^-$ clusters comprise 11 or 12 water molecules. All water molecules are interlinked by hydrogen bonds through 4-, 5- and 6-member rings.

Table 4 shows the β factors at 25 °C calculated for boron isotope substitutions within $B(OH)_3$ and $B(OH)_4^-$ in aqueous solution. For the gas phase calculations, B3LYP methods with and without the D3(BJ) correction provide similar results for β_3 and β_4 factors because there are no weak interactions. In aqueous solution, the β factors converged for the clusters comprising ≥24 water molecules. The effects of hydration lower the β_3 factor by ~4‰, and raise the β_4 factors. Although the B3LYP and B3LYP-D3(BJ) methods give similar β_3 values, the B3LYP-D3(BJ) method increases the β_4 value by an additional ~2‰ compared to the B3LYP method. Because the energy shifts due to boron isotope substitutions are strongly correlated with the stretching vibration modes of B—O bonds (Kowalski et al., 2013), the changes in β factors due to the hydration shell can be qualitatively attributed to the synchronous changes in B—O bond lengths (Table 3).

The α^0_{3-4} values in aqueous solution at 25 °C are shown in Fig. 2.

Table 1
Comparison of β and α factors for boron isotope exchanges between $B(OH)_3$ and $B(OH)_4^-$ in the gas phase calculated at various computational levels.

	β_3				β_4				α^0_{3-4}			
°C	B3LYP[a]	MP2[a]	CCSD(T)[a]	CCSD(T)[b]	B3LYP[a]	MP2[a]	CCSD(T)[a]	CCSD(T)[b]	B3LYP[a]	MP2[a]	CCSD(T)[a]	CCSD(T)[b]
0	1.2666	1.2708	1.2710	1.2729	1.2183	1.2288	1.2305	1.2302	1.0397	1.0342	1.0329	1.0347
5	1.2591	1.2631	1.2634	1.2652	1.2118	1.2220	1.2237	1.2234	1.0390	1.0337	1.0324	1.0341
10	1.2519	1.2558	1.2561	1.2578	1.2056	1.2156	1.2172	1.2169	1.0384	1.0331	1.0319	1.0336
15	1.2450	1.2489	1.2491	1.2508	1.1997	1.2094	1.2110	1.2107	1.0378	1.0326	1.0315	1.0331
20	1.2384	1.2422	1.2424	1.2441	1.1940	1.2035	1.2050	1.2048	1.0372	1.0321	1.0310	1.0326
25	1.2321	1.2358	1.2360	1.2376	1.1886	1.1978	1.1993	1.1991	1.0366	1.0317	1.0305	1.0321
30	1.2260	1.2296	1.2298	1.2314	1.1834	1.1924	1.1939	1.1936	1.0360	1.0312	1.0301	1.0317
35	1.2202	1.2237	1.2239	1.2255	1.1784	1.1872	1.1886	1.1884	1.0354	1.0307	1.0297	1.0312
40	1.2146	1.2180	1.2182	1.2197	1.1736	1.1822	1.1836	1.1833	1.0349	1.0303	1.0292	1.0308
45	1.2092	1.2125	1.2127	1.2142	1.1690	1.1774	1.1787	1.1785	1.0344	1.0299	1.0288	1.0303
50	1.2040	1.2073	1.2075	1.2089	1.1646	1.1727	1.1741	1.1739	1.0338	1.0294	1.0284	1.0299

β_3 is the RPFR of $^{11}B(OH)_3/^{10}B(OH)_3$, β_4 is the RPFR of $^{11}B(OH)_4^-/^{10}B(OH)_4^-$, and $\alpha^0_{3-4}(g)$ is the equilibrium boron isotope fractionation factor between $B(OH)_3$ and $B(OH)_4^-$ in the gas phase calculated using the Bigeleisen-Mayer equation (i.e., $\alpha^0_{3-4}(g) = \beta_3/\beta_4$).

[a] with the 6–311+G(d,p) basis set.

[b] with the aug-cc-pVTZ basis set.

Table 2
Higher-order corrections to β_3, β_4, and α_{3-4} factors at 25 °C calculated for boron isotope exchanges between $B(OH)_3$ and $B(OH)_4^-$ in the gas phase.

25 °C	AnZPE	AnEXC	VrZPE	VrEXC	QmCorr	CenDist	DBOC
β_3	0.9955	0.9999	0.9998	1.0000	1.0000	1.0000	1.0112
β_4	0.9945	0.9998	0.9998	1.0001	1.0000	1.0000	1.0103
α_{3-4}	1.0010	1.0001	1.0000	0.9999	1.0000	1.0000	1.0008

All corrections are calculated at the MP2/6–311+G(d,p) level except for DBOC, which used C-FOUR at the CCSD/pVTZ level. See Section 2.2 for acronyms.

Table 3
Average B—O bond lengths in Å of the dissolved boron species, as a function of the number (n) of solvating water molecules.

Species	Theory level	$n = 0$	$n = 6$	$n = 12$	$n = 18$	$n = 24$	$n = 30$	$n = 36$
$B(OH)_3 \bullet nH_2O$	B3LYP/6–311+G(d,p)	1.370	1.374	1.373	1.373	1.372	1.371	1.371
	B3LYP-D3(BJ)/6–311+G(d,p)	1.369	1.373	1.372	1.371	1.370	1.370	1.370
$B(OH)_4^- \bullet nH_2O$	B3LYP/6–311+G(d,p)	1.487	1.485	1.485	1.483	1.483	1.483	1.483
	B3LYP-D3(BJ)/6–311+G(d,p)	1.486	1.483	1.482	1.480	1.480	1.480	1.480

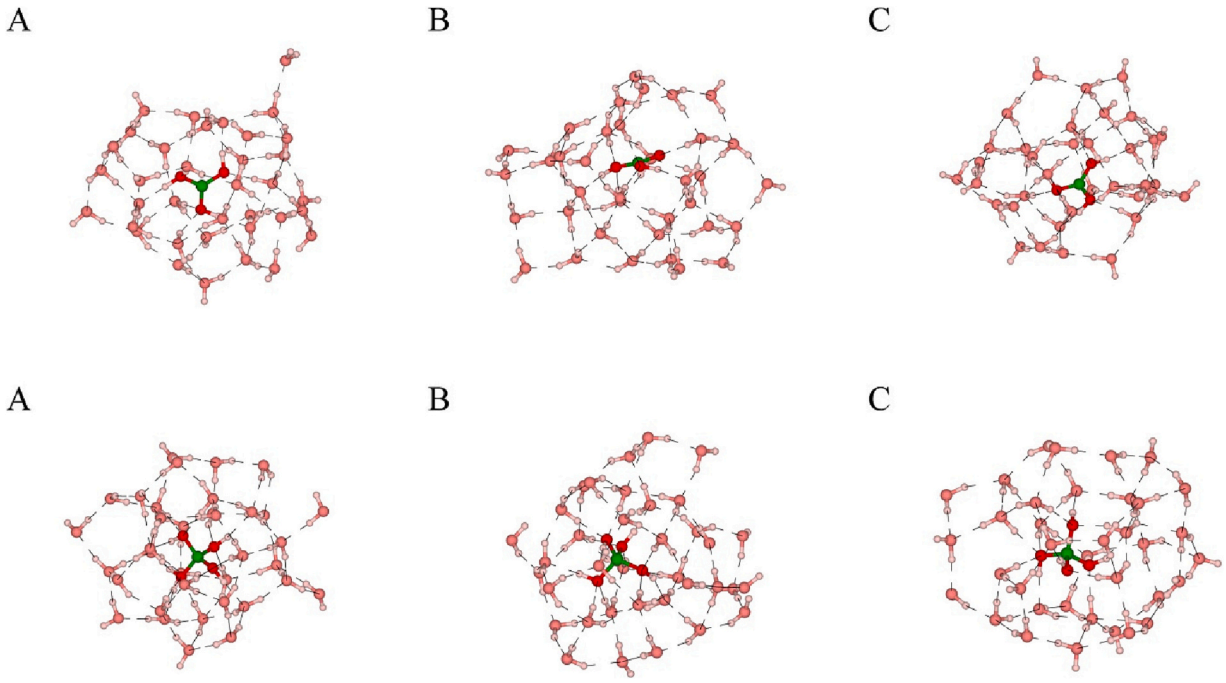

Fig. 1. Configurations of $B(OH)_3$ and $B(OH)_4^-$ species with 36 water molecules in the hydration shell, calculated at B3LYP-D3(BJ)/6–311+G(d,p). Green: boron, red: oxygen, pink: hydrogen, dashed line: hydrogen bond. Upper and lower row configurations are for $B(OH)_3$ and $B(OH)_4^-$ species, respectively, and A, B and C represent three different molecular-cluster configurations. (For interpretation of the references to colour in this figure legend, the reader is referred to the web version of this article.)

Similar to the convergence of β factors, the α^0_{3-4} values converged when $n \geq 24$. At 25 °C, our α^0_{3-4} values in aqueous solution ($n = 36$) are 1.0316 ± 0.0008 and 1.0299 ± 0.0014 for the B3LYP methods without and with the D3(BJ) correction, respectively. These results are in good agreement with the previous studies of Rustad et al. (2010) and Li et al. (2020), who used ab initio molecular dynamics to obtain the configurations in explicit water. This means that the different approaches of simulating aqueous environments can yield similar results for studies of isotope fractionation in aqueous solution. Because our α^0_{3-4} values in aqueous solution are similar when $n > 24$, the results of $n = 36$ were selected for further calculation of solvation effects.

4. Discussion

4.1. The effect of ion pairs in seawater

In seawater, $B(OH)_4^-$ can form ion pairs with Na^+, Mg^{2+} and Ca^{2+}, such ion pairs account for about 44% of total borate ions (Byrne and Kester, 1974). Because the mean value of α_{3-4} in pure water at 25 °C measured by Klochko et al. (2006) was ~4‰ larger than that of seawater, it is valuable to evaluate whether ion pairs could affect the determination of α_{3-4} in seawater. Table 5 shows the β_4 values of the ion paired $B(OH)_4^-$ with Na^+, Mg^{2+} and Ca^{2+} calculated at the B3LYP-D3(BJ)/6–311+G(d,p) level for 25 °C. The β_4 values show consistent results when $n \geq 24$, suggesting that the hydration shell used here reaches a simulation quality for presenting solvation effects on the β factors (Table A1). We substituted Na^+ with Mg^{2+} or Ca^{2+} in the cluster of $NaB(OH)_4$ with 36 water molecules to build the cluster of $MgB(OH)_4^+$ and $CaB(OH)_4^+$ due to the similar ionic radii of these cations, and optimized the clusters of $MgB(OH)_4^+$ and $CaB(OH)_4^+$ with 36 water molecules for frequency analyses. When $n = 36$, the average β_4 factors of Na^+, Mg^{2+}, and Ca^{2+} paired $B(OH)_4^-$ are 1.1937 ± 0.0009, 1.1931 ± 0.0010, and 1.1929 ± 0.0019 at 25 °C, which are consistent with the β_4 factor of $B(OH)_4^-$ (1.1927 ± 0.0009) within the computational uncertainties.

Table 4
Comparison of β factors calculated for aqueous solution at the B3LYP/6–311+G(d,p) level with and without the D3 Landon-dispersion correction at 25 °C.

	Theory level		$n = 0$	$n = 6$	$n = 12$	$n = 18$	$n = 24$	$n = 30$	$n = 36$
β_3	B3LYP/6–311+G(d,p)	A	1.2321	1.2275	1.2278	1.2272	1.2278	1.2278	1.2284
		B	1.2321	1.2283	1.2263	1.2268	1.2284	1.2296	1.2273
		C	1.2321	1.2281	1.2282	1.2278	1.2288	1.2285	1.2289
		Ave.	1.2321	1.2280	1.2275	1.2273	1.2283	1.2286	1.2282
	B3LYP-D3(BJ)/6–311+G(d,p)	A	1.2323	1.2283	1.2283	1.2283	1.2280	1.2266	1.2265
		B	1.2323	1.2291	1.2272	1.2277	1.2308	1.2297	1.2293
		C	1.2323	1.2287	1.2291	1.2284	1.2269	1.2280	1.2293
		Ave.	1.2323	1.2287	1.2282	1.2281	1.2285	1.2281	1.2284
β_4	B3LYP/6–311+G(d,p)	A	1.1886	1.1908	1.1906	1.1912	1.1903	1.1899	1.1904
		B	1.1886	1.1908	1.1887	1.1905	1.1902	1.1918	1.1913
		C	1.1886	1.1904	1.1905	1.1899	1.1903	1.1898	1.1898
		Ave.	1.1886	1.1906	1.1900	1.1905	1.1902	1.1905	1.1905
	B3LYP-D3(BJ)/6–311+G(d,p)	A	1.1891	1.1922	1.1926	1.1934	1.1933	1.1927	1.1928
		B	1.1891	1.1922	1.1903	1.1934	1.1927	1.1939	1.1938
		C	1.1891	1.1917	1.1920	1.1910	1.1919	1.1919	1.1915
		Ave.	1.1891	1.1920	1.1916	1.1926	1.1927	1.1928	1.1927

n is the number of water molecules used to simulate the hydration shells. A, B, and C represent the three different model configurations. Ave. is the arithmetic mean of A, B, and C.

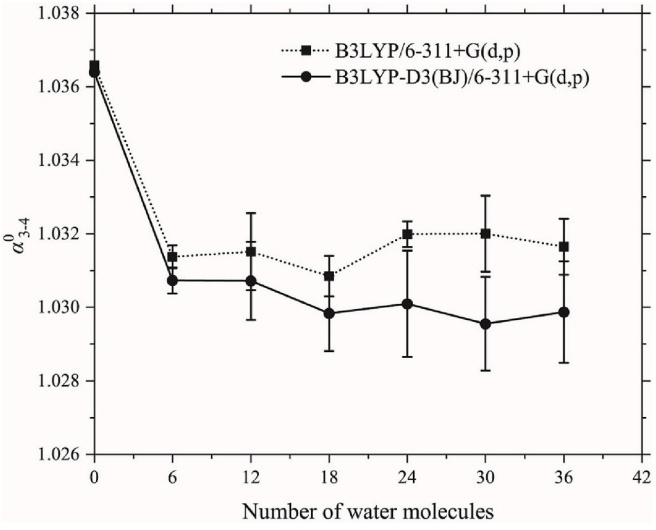

Fig. 2. Comparison of α^0_{3-4} values in aqueous solution calculated from the B3LYP method with and without the D3 London dispersion correction.

Table 5
β_4 factors calculated for the ion paired $B(OH)_4^-$ in aqueous solution at 25 °C, using B3LYP-D3(BJ)/6–311+G(d,p).

Ion pair	A	B	C	Ave.
$NaB(OH)_4 \bullet 36H_2O$	1.1927	1.1949	1.1935	1.1937
$MgB(OH)_4^+ \bullet 36H_2O$	1.1922	1.1944	1.1926	1.1931
$CaB(OH)_4^+ \bullet 36H_2O$	1.1932	1.1950	1.1904	1.1929

A, B, and C represent the three different model configurations. Ave. is the arithmetic mean of A, B, and C.

According to the study of Byrne and Kester (1974), the ion pairs of $NaB(OH)_4$, $MgB(OH)_4^+$, and $CaB(OH)_4^+$ in seawater at 25 °C, a salinity of 34.8 ‰, and pH = 8.2 are 3.6 ± 0.4%, 5.1 ± 0.4%, and 1.6 ± 0.2% of the total boron, while the proportions of $B(OH)_3$ and $B(OH)_4^-$ are 76.4 ± 1.0%, and 13.3 ± 0.6%, respectively. If we consider the contribution of ion paired boron species, the overall β_4 factor in seawater would be ~1.1929 at 25 °C, almost identical to the β_4 factor of $B(OH)_4^-$ in pure water. Therefore, our calculation suggests that the α_{3-4} values in seawater and pure water would be almost identical. However, we noted that the β_4 factor of $NaB(OH)_4$ was statistically larger than that of $B(OH)_4^-$ by ~1‰ within the computational error. Recently, Henehan et al. (2022) postulated the importance of ion pairs of boron species during boron incorporation into calcite and aragonite, and suggested that $NaB(OH)_4$ can substitute into the carbonate lattice to balance the local charge. Our results imply that the ion pair of $NaB(OH)_4$ would only make minor contributions (up to ~1‰) to the boron isotope effects during boron incorporation into marine carbonates if isotopic equilibrium is achieved.

4.2. Contribution of solvation effects

Table 6 shows our calculation of the solvation effects on α_{3-4} at 25 °C. Because of solvation effects, the equilibrium boron isotope fractionation factor in aqueous solution differs from that in the gas phase (Rustad et al., 2010). The solvation effects in aqueous solution are mainly manifested in solute−water interactions that are affected by Coulombic interaction, repulsion, polarization, dispersion, and hydrogen bonding (Kubicki, 2016). Compared to implicit solvent models, simulations in explicit water generally provide a better description of intermolecular interactions, especially when hydrogen bonding is significant (Kannath et al., 2020). As it is unrealistic to adopt CCSD(T) in explicit solvent models, the application of DFT becomes the most practicable approach for such calculations. However, conventional Kohn-Sham density functional theory (KS-DFT) does not properly describe long-range London dispersion interactions, and may fail to provide reliable interaction

Table 6
Estimation of the contribution of solvation effects to α_{3-4} compared to the results of Li et al. (2020) at 25 °C.

Theory level	$\alpha^0_{3-4}(g)$	$\alpha^0_{3-4}(l)$	K^{solv}	Notes
B3LYP/6-31G(d)	1.0287	1.0270	0.9983	Li et al. (2020)
B3LYP/6–311G(d,p)	1.0323	1.0296	0.9974	Li et al. (2020)
B3LYP/6–311+G(d,p)	1.0367	1.0324	0.9959	Li et al. (2020)
B3LYP/6–311+G(d,p)	1.0366	1.0316	0.9952	This study
B3LYP-D3/6-31G(d)	1.0287	1.0227	0.9942	Li et al. (2020)
B3LYP-D3(BJ)/6-311G(d,p)	1.0323	1.0254	0.9933	Li et al. (2020)
B3LYP-D3(BJ)/6-311+G(d,p)	1.0367	1.0303	0.9938	Li et al. (2020)
B3LYP-D3(BJ)/6-311+G(d,p)	1.0364	1.0299	0.9937	This study

$\alpha^0_{3-4}(g)$ or $\alpha^0_{3-4}(l)$ is the equilibrium boron isotope fractionation factor between $B(OH)_3$ and $B(OH)_4^-$ in the gas (g) or liquid (l) phase calculated using the Bigeleisen-Mayer equation. The $\alpha^0_{3-4}(l)$ values with 36 water molecules were selected for comparison. K^{solv} is the contribution of solvation effects to the equilibrium constant (i.e., $K^{solv} = \alpha^0_{3-4}(l)/\alpha^0_{3-4}(g)$). Note, the K^{solv} values of Li et al. (2020) were recalculated using their data, and are consistent between different basis sets under the B3LYP-D3 method. However, the $\alpha^0_{3-4}(l)$ value from the B3LYP-D3 method can be significantly lower than the experimental observations when using a small basis set such as 6-31G(d).

potentials (Grimme, 2011). Therefore, London dispersion corrected DFT methods are recommended to overcome the deficiency of KS-DFT. Of the current dispersion-corrected DFT methods, the DFT-D3 approach is the recommended method to study large systems, because of its efficient treatment of London dispersion interactions (Grimme, 2012). London dispersion is an electron-correlation effect that improves the calculation of potential energy surfaces, and influences the calculation of geometries and frequencies. As accurate determination of geometries and frequencies is key to obtaining reliable equilibrium isotope fractionation factors, application of the DFT-D3 method will improve the accuracy of calculating $\alpha_{3\text{–}4}$ values in aqueous solution. Therefore, we used results of our B3LYP-D3(BJ)/6–311+G(d,p) calculations to calculate solvation effects, which reduced the $\alpha_{3\text{–}4}$ at 25 °C by ~6‰.

Using various DFT and MP2 methods, Rustad et al. (2010) systematically evaluated solvation effects on predicting $\alpha_{3\text{–}4}$ values at 25 °C, they found that explicit solvation with 32 water molecules reduced $\alpha_{3\text{–}4}$ value by ~3–5‰. Although Rustad et al. (2010) noted that DFT functionals cannot properly describe hydrogen bonding and dispersion, they did not compensate for such shortcomings. As the MP2 methods are better than DFT methods at describing weak interactions, Rustad et al. (2010) extrapolated the $\alpha_{3\text{–}4}$ values from MP2/aug-cc-pVTZ calculations to be 1.026–1.028; the extrapolation combined the solvation effects of the inner hydrogen shell of MP2 (n = 8–11) and the outer hydrogen shell of DFT (n = 11–32). These values agree with the measured $\alpha_{3\text{–}4}$ for seawater. Agreement benefits from 4 aspects: (1) when calculating isotope fractionation factors in solution, the effect of the inner hydrogen shell is more important than the outer hydrogen shell, (2) $\alpha_{3\text{–}4}$ values in the gas phase are closer to the true value when calculated from MP2 methods rather than from DFT, (3) computational errors cancel out the effects of anharmonicity and DBOC, and (4) ion pairs show minor influences on boron isotope fractionation. Rustad et al. (2010) evaluated the computational errors of various DFT and MP2 models; however, it was a computationally expensive approach for calculating isotope effects in solution. Furthermore, Rustad et al. (2010) did not explain their extrapolation theory, limiting similar extrapolation to other solution systems. In contrast, our strategy allows solvation effects to be calculated in a simple and understandable way. If we consider the contribution of higher-order corrections, solvation effects should reduce $\alpha_{3\text{–}4}$ by ~5–7‰ in the calculations of Rustad et al. (2010).

Recently, Li et al. (2020) compared various basis sets using the B3LYP functional; they showed that the B3LYP/6-31G(d) level produced an $\alpha_{3\text{–}4}$ value in aqueous solution close to the experimental values. Consequently, Li et al. (2020) employed B3LYP/6-31G(d) to investigate boron isotope fractionation between tourmaline group minerals and fluids; they argued that the absence of diffusive functions in the basis set can yield better results through error cancellation. However, the agreement between the results of B3LYP/6-31G(d) and the experimental measurements could be fortuitous. Indeed, doubts about the usefulness of B3LYP/6-31G(d) have been raised in the past, and the using a D3 correction on the B3LYP/6-31G(d) level would improve predictions of thermodynamic properties without significant additional computational cost (Kruse et al., 2012). Table 6 compares our results to the solvation effects recalculated using the data of Li et al. (2020) with and without D3 corrections. The K^{solv} values are relatively consistent when the D3 correction was employed but are more varied for the models without the D3 correction. Notably, as the basis set is increased from 6–31G(d) to 6–311+G(d,p), the K^{solv} values without the D3 correction approach the K^{solv} values with the D3 correction. This trend can also be extracted from the data of Rustad et al. (2010); for example, the K^{solv} value generated from the B3LYP/aug-cc-pVDZ level is 0.9953, closer to our K^{solv} value with the D3 correction (B3LYP-D3(BJ)/6–311+G(d,p) = 0.9937) than that of B3LYP/6-31G(d) (0.9983). This finding suggests: (1) although solvation effects may not be reproduced accurately, D3-uncorrected DFT methods can provide a good description of solvation effects when in combination with the complete basis set limit, and (2) D3-corrected DFT methods provide reasonable descriptions of solvation effects even with lower-level basis sets.

Zeebe and Rae (2020) calculated $\alpha_{3\text{–}4}$ values using the X3LYP/6–311+G(d,p) theory level, and found that solvation effects reduce the $\alpha_{3\text{–}4}$ value at 25 °C by ~6‰. X3LYP has a better description of weak interactions than D3-uncorrected B3LYP (Xu and Goddard, 2004; Grimme, 2011); therefore, it is not surprising that the effect of solvation on the $\alpha_{3\text{–}4}$ value estimated by Zeebe and Rae (2020) is similar to our prediction using the B3LYP-D3(BJ) method. However, the $\alpha_{3\text{–}4}$ value in aqueous solution calculated by Zeebe and Rae (2020) is ~30‰ at 25 °C, which is larger than the experimental determinations. Even if solvation effects can be better estimated by introducing a proper description of weak interactions, the physicochemical properties of the boron species (e.g., zero-point energies) still cannot be obtained accurately from DFT alone. Therefore, robust computation of energy shifts in the gas phase provides a better guarantee of accurate predictions of isotope fractionation factors in solutions. This can also explain why Li et al. (2020) obtained an $\alpha_{3\text{–}4}$ value in agreement with the experimental observations by using B3LYP/6-31G(d). Their calculated $\alpha_{3\text{–}4}$ value in the gas phase is 1.0287, which is fortuitously close to the experimental values for the liquid phase when the calculation of solvation effects is close to 1.

Based on comparisons with previous studies, we are confident that the application of the DFT-D3 method can benefit the calculations of isotope effects in solution, especially solvation effects. We found that solvation effects play an important role in the calculation of $\alpha_{3\text{–}4}$ values, which contribute approximately −6‰ to the $\alpha_{3\text{–}4}$ value at room temperature.

4.3. Temperature dependence of the $\alpha_{3\text{–}4}$ value in aqueous solution

Once $\alpha^{0}_{3\text{–}4}$ values in the gas phase, correction terms, and the contributions of solvation effects are accurately calculated, reliable $\alpha_{3\text{–}4}$ values in aqueous solution can be calculated from Eq. (12). Fig. 3 compares our calculated $\alpha_{3\text{–}4}$ values in aqueous solution with experimental observations, and shows the temperature dependence of $\alpha_{3\text{–}4}$ values between 0 and 50 °C (the $\alpha_{3\text{–}4}$ values in aqueous solution can be found in Table A2). At 25 °C, our calculated $\alpha_{3\text{–}4}$ value was 1.0275, from CCSD(T)/aug-cc-pVTZ level, which is almost identical to the experimental result (1.0272 ± 0.0006) of Klochko et al. (2006). Our $\alpha_{3\text{–}4}$ value was 1.0259, from CCSD(T)/6–311+G(d,p) level at 25 °C, which is almost identical to the result (1.026 ± 0.001) of Nir et al. (2015). At 40 °C, our calculated $\alpha_{3\text{–}4}$ values (1.0264 and 1.0249 from CCSD(T)/aug-cc-pVTZ and CCSD(T)/6–311+G(d,p) levels, respectively) are lower than the measurement (1.0289 ± 0.0048) of Klochko et al. (2006) for pure water; however, our values are within their uncertainty (Fig. 3). As temperature increases from 0 to 50 °C, our $\alpha_{3\text{–}4}$ values in aqueous solution decrease from 1.0295 to 1.0257 for the CCSD(T)/aug-cc-pVTZ level, and from 1.0278 to 1.0242 for the CCSD(T)/6–311+G(d,p) level. Both theoretical treatments show a decrease of ~4‰ for the temperature range studied here, which is consistent with thermodynamic principles.

The temperature effect of $\alpha_{3\text{–}4}$ may have potential implications for either calibrating $\delta^{11}B$ values of aqueous borate or reconstructing paleo-pH and paleo-pCO_2 (Hönisch et al., 2008). Henehan et al. (2016) provided an open-ocean calibration of the planktic foraminifera *Orbulina universa* grown at various temperatures (9.0–27.9 °C) to obtain the $\delta^{11}B$ values of borate in ambient water. The planktic foraminifera tended to record lower $\delta^{11}B$ values at lower temperatures, which means that the temperature of the ocean would affect the boron isotope records of biogenic or inorganic carbonates through the temperature dependences of pK^*_B and $\alpha_{3\text{–}4}$. In modern seawater with pH = 8.2 and Salinity = 35, according to the results of Dickson (1990) and this study, the temperature effects on pK^*_B and $\alpha_{3\text{–}4}$ contribute ~75% and ~ 25% of the total change in $\delta^{11}B$ of aqueous borate, respectively, for a temperature change of 5 °C from room temperature (see the supplementary file). Therefore, it is necessary to use a temperature-corrected $\alpha_{3\text{–}4}$ rather than a constant to calibrate $\delta^{11}B$ values of aqueous borate. Although Henehan et al. (2016) found that the $\delta^{11}B$ values of *Orbulina universa* showed no

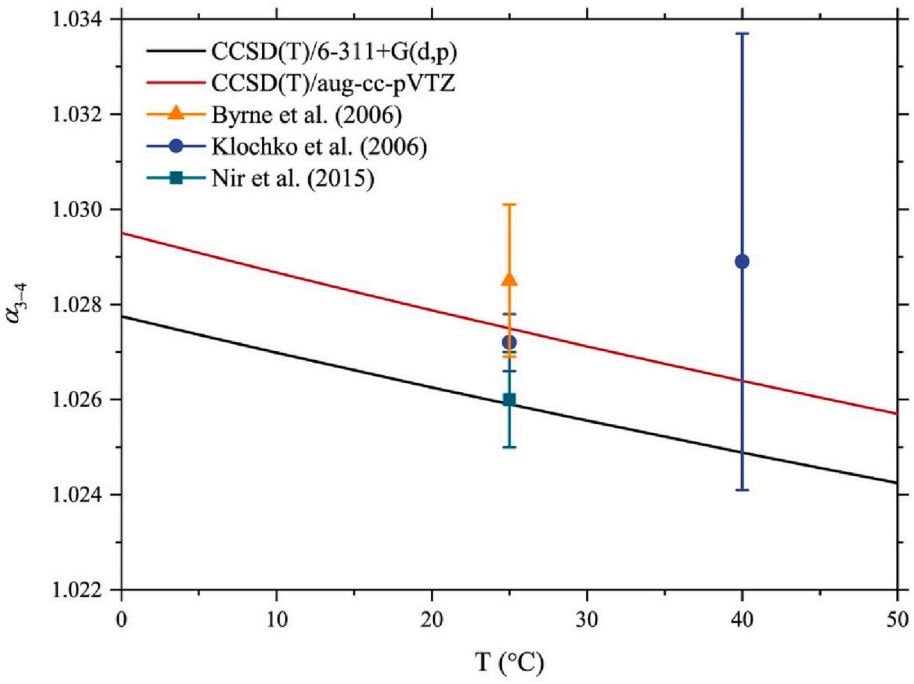

Fig. 3. Comparison of α_{3-4} values in aqueous solution across a range of temperatures (0–50 °C) determined by theoretical calculations and experimental measurements. Note that the results for pure water in Klochko et al. (2006) are selected for the comparison at 40 °C. The black line is our results based on the calculation of CCSD(T)/aug-cc-pVTZ, showing a linear fitting against temperature as α_{3-4} = 1.02944–7.59673 × 10^{-5} T (T: 0–50 °C). The red line is our results based on the calculation of CCSD(T)/6–311+G(d,p), showing α_{3-4} = 1.02769–7.00982 × 10^{-5} T (T: 0–50 °C). (For interpretation of the references to colour in this figure legend, the reader is referred to the web version of this article.)

correlation between their offsets from aqueous borate and ambient temperature (which are related to the mechanism of boron isotope fractionation between carbonates and fluids), Hönisch et al. (2019) found that the slope of the open-ocean calibration of Henehan et al. (2016) can be more consistent with the laboratory calibrations for *Orbulina universa* if a temperature-corrected α_{3-4} was employed. The similarity of the two calibrations also suggests that the temperature effect on α_{3-4} may have potential for better understanding the boron isotope paleo-pH proxy, and our results provide a robust estimation of the temperature dependence of α_{3-4} for further investigations. For reconstructing pH and pCO_2, the temperature effect on α_{3-4} has a relatively small contribution compared to other uncertainties (Rae et al., 2011). For example, Hönisch et al. (2019) found that the influence of temperature changes within 3 °C did not exceed the average pH and pCO_2 uncertainty. Therefore, Hönisch et al. (2019) recommended using a temperature-corrected α_{3-4} to reconstruct the paleo-pH of the ocean rather than a constant α_{3-4} value only if the change in ocean temperature is >5 °C (i.e., an ~0.35‰ change in our calculated α_{3-4}).

Theoretically, the CCSD(T)/aug-cc-pVTZ level provides more reliable molecular constants than CCSD(T)/6–311+G(d,p), but that may not always be so. Since the difference between the zero-point energy shifts calculated by the two CCSD(T) methods is only 0.2 cm^{-1} for the boron isotope substitution in $B(OH)_3$, it is difficult for us to evaluate whether the 0.2 cm^{-1} difference is due to an improvement by using aug-cc-pVTZ in the neutral system. Considering our calculations, the results from CCSD(T)/aug-cc-pVTZ and CCSD(T)/6–311+G(d,p) are similar and are in good agreement with the experimental measurements; therefore, we cannot distinguish which theory level is more accurate. However, the α_{3-4} value of 1.026 at 25 °C, matches the aragonite precipitate values of Noireaux et al. (2015) and Henehan et al. (2022). From this agreement, we cannot infer that a value of 1.026 for α_{3-4} is more accurate because $NaB(OH)_4$ ion pair may play a role in aragonite precipitation (Mavromatis et al., 2021; Henehan et al., 2022). If $NaB(OH)_4$ in solution is more enriched in ^{11}B than $B(OH)_4$ by ~1‰, as we calculated, it may suggest that the fitting results of Noireaux et al. (2015) and Henehan et al. (2022) arise from the incorporation of $NaB(OH)_4$ in aragonite. If so, then α_{3-4} in seawater should be slightly larger than 1.026, ~1.027‰. Further first-principles calculations of boron isotope effects associated with surface reactions of carbonates may provide a clue to this issue.

4.4. Uncertainties of α_{3-4} values

The uncertainties of our α_{3-4} values between $B(OH)_3$ and $B(OH)_4^-$ in aqueous solution are affected by: (1) the uncertainty of α^0_{3-4} values in the gas phase, (2) the uncertainty of high-order corrections, and (3) the uncertainty arising from the hydration shell. Error propagation from the three sources of uncertainly can be used to estimate the uncertainty of our α_{3-4} values in aqueous solution. To estimate the uncertainty of α^0_{3-4} values in the gas phase, data from different theoretical methods and basis sets should be compared. Typically, the influence of the theoretical methods is greater than that of the basis sets, which explains why the α^0_{3-4} values obtained from B3LYP/6–311+G(d,p) have a discrepancy of ~6‰ from those of CCSD(T)/6–311+G(d,p) in Table 1. If the basis sets used are close to the complete basis set limit, then α values calculated from different basis sets should be similar for the same theoretical method, which was the case for our α^0_{3-4} values with the CCSD(T) methods. Therefore, the uncertainty of our α^0_{3-4} values in the gas phase from the CCSD(T) methods can be estimated from the difference between the α^0_{3-4} values calculated from the CCSD(T)/6–311+G(d,p) and CCSD(T)/aug-cc-pVTZ levels, which would be within ±0.0016 at room temperature.

Considering the higher-order corrections, AnZPE and DBOC play important roles in improving the accuracy of α_{3-4} values by ~1.8‰. Compared with the vibrational energy shifts due to boron isotope substitutions, the contributions of AnZPE and DBOC are small when calculating the α_{3-4} values. Although the higher-order corrections have small numerical errors, the uncertainty in AnZPE and DBOC can be considered negligible because the error terms cancel out when the α_{3-4} values are calculated (Liu and Liu, 2016; Liu et al., 2021). As aqueous solutions are complex, solvation effects also contribute to the uncertainties. From the variations in our β values, the computational uncertainties of α^0_{3-4} values in aqueous solution are ~ ± 0.0005 (95% confidence interval) under the B3LYP method and ~ ±0.0010 (95% confidence interval) under the B3LYP-D3(BJ) method. However, considering the consistency in the mean values of the K^{solv} corrections calculated with different basis sets and the B3LYP-D3(BJ) method (Table 6), the uncertainty in our K^{solv} values is ±0.0005 for boron

isotope exchanges in aqueous solution. If we adopt ±0.0005 as the uncertainty in the calculated solvation effects, then the uncertainty of our predicted α_{3-4} values in aqueous solution should be within ±0.0017.

4.5. Geochemical applications

The theoretical calculations of this work provide accurate α_{3-4} values in aqueous solution, and accurate β factors for dissolved boron species (Fig. A2). The β factors are valuable for further evaluating boron isotope fractionation between solids (or solid surfaces) and fluids. Balan et al. (2018) calculated β factors of structural boron atoms in calcite and aragonite; additionally, they evaluated boron isotope fractionation between carbonates and aqueous solution based on the β factors of $B(OH)_3$ and $B(OH)_4^-$ calculated by Rustad et al. (2010). Using our updated β factors, the boron isotope fractionation between carbonates and the liquid in the Balan et al. (2018) study should decrease by ~1.7‰ and ~2.6‰ for the trigonal and tetrahedral boron species at room temperature, respectively. For example, at 300 K, the equilibrium boron isotope fractionation would be ~12.8‰ between the two trigonal boron species in calcite and aqueous $B(OH)_3$, and ~ 7.2‰ between the tetrahedral boron species in aragonite and aqueous $B(OH)_4^-$.

Mavromatis et al. (2021) conducted synthetic experiments to form carbonates via an amorphous calcium carbonate (ACC) pathway, and found that boron isotope fractionation between aragonite and aqueous $B(OH)_4^-$ is 6.7 ± 1.3‰ at 25 °C. This value is in excellent agreement with our prediction of ~7.2‰, which supports the statement of Mavromatis et al. (2021) that the transformation of ACC precursors to aragonite is likely to lead to equilibrium boron isotope fractionation between solids and fluids. In contrast to the ^{11}B enrichment of aragonite measured by Mavromatis et al. (2021), Noireaux et al. (2015) observed almost no boron isotope fractionation between aragonite and aqueous $B(OH)_4^-$ during classical growth of carbonates. The tetrahedral boron species in aragonites were 40–50% and > 90% of the total structural boron atoms in the studies of Mavromatis et al. (2021) and Noireaux et al. (2015), respectively. Based on our results, an explanation is that more tetrahedral boron species were dehydroxylated to trigonal coordination during the ACC pathway, and that boron adsorption onto the aragonite surface controls the isotope effects during classical growth processes rather than equilibrium isotope fractionation. Using our data, the theoretical prediction of isotope fractionation between the tetrahedral boron in calcite and aqueous $B(OH)_4^-$ of Balan et al. (2018) would be 9.8‰ at room temperature. The offsets between $\delta^{11}B$ in calcite and $\delta^{11}B$ of borate observed by Noireaux et al. (2015) are 7.8–10.6‰ at around pH 7.5. The measured boron isotope fractionation at low pH is also close to the equilibrium isotope fractionation results. The experiments of Saldi et al. (2018) suggest that only $B(OH)_4^-$ is adsorbed onto inorganic calcite at near-equilibrium conditions. Thus, the agreement between our results and the experimental observations at around pH 7.5 suggests that the signatures of ^{11}B enrichments in calcite minerals may also represent the incorporation of $B(OH)_4^-$ at near-equilibrium conditions. With increasing pH, the offsets between $\delta^{11}B$ in calcite and $\delta^{11}B$ in borate decrease significantly. For example, following the classical growth of calcite at pH ≈ 9, the offset is ~4‰ in Noireaux et al. (2015) and 0 ± 1‰ in Kaczmarek et al. (2016), and ~ −0.8 ± 2.9‰ in Mavromatis et al. (2021) for the ACC pathway. As the ratio of $B(OH)_4^-$ to $B(OH)_3$ increases with increasing pH, Mavromatis et al. (2021) reasoned that changes in aqueous speciation, such as an increase in $NaB(OH)_4$, may be responsible for the isotopic changes. From our calculation at equilibrium conditions, significant isotope changes over a broad pH range cannot be attributed to the $NaB(OH)_4$ ion pair, because the boron isotope composition of $NaB(OH)_4$ is very similar to $B(OH)_4^-$. Instead, at high pH, kinetic isotope fractionation during boron incorporation into calcites is expected. Isotope equilibrium means that the forward and backward reaction rates are equal for an isotope exchange reaction. If boron isotope exchange between carbonates and fluids is out of equilibrium (for example, arising from changes in aqueous chemistry), then attachment or detachment of boron species during $CaCO_3$ precipitation may dominate the boron isotope exchange reactions. In general, the B/Ca ratio of carbonates increases with increasing aqueous pH, and the B/Ca ratio of aragonite is greater than that of calcite (e.g., Henehan et al., 2022). If higher B/Ca ratio of carbonates corresponds to higher boron incorporation rates (i.e., incorporation versus the reverse desorption reaction), then the forward reaction (i.e., adsorption of $B(OH)_4^-$ onto carbonate, followed by uptake into the lattice) may dominate the boron isotope exchange reaction. Therefore, it is probable that the observed changes in boron isotope fractionation in calcites at higher pH result from fast boron incorporation rates (not $CaCO_3$ precipitation rates, Noireaux et al., 2015; Mavromatis et al., 2015; Farmer et al., 2019).

5. Conclusions

This work proposed a theoretical strategy for improving the calculation of isotopic fractionation between species in aqueous solution. Based on our strategy, accurate boron isotope fractionation factors between dissolved boron species were determined beyond the RRHO and BO approximations. Benchmark results from CCSD(T) are presented for equilibrium boron isotope fractionation between gaseous $B(OH)_3$ and $B(OH)_4^-$. The effects of anharmonicity and diagonal Born−Oppenheimer correction were found to be important for improving the calculation of β factors of boron species. For example, the contribution of anharmonicity reduces the β_3 value by ~5.6‰ at 25 °C. At room temperature, the contributions of higher-order corrections raise the α_{3-4} values by ~2‰, and solvation effects lower the α_{3-4} values by ~6‰. Our predictions show that the α_{3-4} value in aqueous solution should be 1.0259–1.0275 at 25 °C, which is in excellent agreement with the experimental measurements of Nir et al. (2015) and Klochko et al. (2006). The dependence of the α_{3-4} values on temperature was found to decrease by ~4‰ from 0 to 50 °C. Ion pairs of $B(OH)_4^-$ and cations (Na^+, Mg^{2+}, and Ca^{2+}) were found to carry a boron isotope signature similar to that of $B(OH)_4^-$ in aqueous solution. Therefore, boron isotope fractionation between $B(OH)_3$ and $B(OH)_4^-$ should be almost identical in seawater and pure water, and ion pairs would have minor effects on boron isotope fractionation between carbonates and aqueous $B(OH)_4^-$ under near-equilibrium conditions. However, further first-principles calculations examining the effect of ion pairs adsorbed onto carbonates are necessary to understand the correlation between Na and B incorporation into carbonates as found by Henehan et al. (2022). In addition, our calculations provide accurate β factors of boron species in aqueous solution, which are valuable for understanding the boron isotope fractionation associated with the liquid phase; for example, boron isotope fractionation between minerals (or mineral surfaces) and dissolved boron species.

Declaration of Competing Interest

The authors declare that they have no known competing financial interests or personal relationships that could have appeared to influence the work reported in this paper.

Data availability

We have shared the research data in the supplementary file.

Acknowledgments

This work is supported by the Strategic Priority Research Program of Chinese Academy of Sciences (XDB 41000000), National Natural Science Foundation of China (42130114, 41903019, 41773016, 41603015), Pre-research Project on Civil Aerospace Technologies No. D020202 funded by Chinese National Space Administration, and the Frontier Project of State Key Laboratory of Ore-deposit Geochemistry, Chinese Academy of Sciences (202105). We thank Michael J. Henehan

and two anonymous reviewers for their constructive comments on this manuscript.

Appendix A. Supplementary data

Supplementary data to this article can be found online at https://doi.org/10.1016/j.chemgeo.2023.121455.

References

Anbar, A.D., Jarzecki, A.A., Spiro, T.G., 2005. Theoretical investigation of iron isotope fractionation between $Fe(H_2O)_6^{3+}$ and $Fe(H_2O)_6^{2+}$: implications for iron stable isotope geochemistry. Geochim. Cosmochim. Acta 69, 825–837. https://doi.org/10.1016/j.gca.2004.06.012.

Balan, E., Noireaux, J., Mavromatis, V., Saldi, G.D., Montouillout, V., Blanchard, M., Pietrucci, F., Gervais, C., Rustad, J.R., Schott, J., Gaillardet, J., 2018. Theoretical isotopic fractionation between structural boron in carbonates and aqueous boric acid and borate ion. Geochim. Cosmochim. Acta 222, 117–129. https://doi.org/10.1016/j.gca.2017.10.017.

Becke, A.D., 1993. Density-functional thermochemistry. III. The role of exact exchange. J. Chem. Phys. 98, 5648–5652. https://doi.org/10.1063/1.464913.

Becke, A.D., Johnson, E.R., 2005. A density-functional model of the dispersion interaction. J. Chem. Phys. 123, 154101 https://doi.org/10.1063/1.2065267.

Bigeleisen, J., 1996. Nuclear size and shape effects in chemical reactions. Isotope chemistry of the heavy elements. J. Am. Chem. Soc. 118, 3676–3680. https://doi.org/10.1021/ja954076k.

Bigeleisen, J., Mayer, M.G., 1947. Calculation of equilibrium constants for isotopic exchange reactions. J. Chem. Phys. 15, 261–267. https://doi.org/10.1063/1.1746492.

Blanchard, M., Dauphas, N., Hu, M.Y., Roskosz, M., Alp, E.E., Golden, D.C., Sio, C.K., Tissot, F.L.H., Zhao, J., Gao, L., Morris, R.V., Fornace, M., Floris, A., Lazzeri, M., Balan, E., 2015. Reduced partition function ratios of iron and oxygen in goethite. Geochim. Cosmochim. Acta 151, 19–33. https://doi.org/10.1016/j.gca.2014.12.006.

Bron, J., Chang, C.F., Wolfsberg, M., 1973. Isotopic partition function ratios involving H_2, H_2O, H_2S, H_2Se, and NH_3. Z. Naturforsch. A 28, 129–136. https://doi.org/10.1515/zna-1973-0203.

Byrne, R.H., Kester, D.R., 1974. Inorganic speciation of boron in seawater. J. Mar. Res. 32, 119–127.

Byrne, R.H., Yao, W.S., Klochko, K., Tossell, J.A., Kaufman, A.J., 2006. Experimental evaluation of the isotopic exchange equilibrium $^{10}B(OH)_3 + {}^{11}B(OH)_4^- = {}^{11}B(OH)_3 + {}^{10}B(OH)_4^-$ in aqueous solution. Deep Sea Res. Part I Oceanogr. Res. Pap. 53, 684–688. https://doi.org/10.1016/j.dsr.2006.01.005.

CFOUR, 2000. A quantum chemical program package written by J.F. Stanton, J. Gauss, L. Cheng, M.E. Harding, D.A. Matthews, P.G. Szalay with contributions from A.A. Auer, R.J. Bartlett, U. Benedikt, C. Berger, D.E. Bernholdt, Y.J. Bomble, O. Christiansen, F. Engel, R. Faber, M. Heckert, O. Heun, C. Huber, T.-C. Jagau, D. Jonsson, J. Jusélius, K. Klein, W.J. Lauderdale, F. Lipparini, T. Metzroth, L.A. Mück, D.P. O'Neill, D.R. Price, E. Prochnow, C. Puzzarini, K. Ruud, F. Schiffmann, W. Schwalbach, C. Simmons, S. Stopkowicz, A. Tajti, J. Vázquez, F. Wang, J.D. Watts and the integral packages MOLECULE (J. Almlöf and P.R. Taylor), PROPS (P.R. Taylor), ABACUS (T. Helgaker, H.J. Aa. Jensen, P. Jørgensen, and J. Olsen), and ECP routines by A. V. Mitin and C. van Wüllen. For the current version. see. http://www.cfour.de.

Chen, X., Regan, C.K., Craig, S.L., Krenske, E.H., Houk, K., Jorgensen, W.L., Brauman, J. I., 2009. Steric and solvation effects in ionic SN2 reactions. J. Am. Chem. Soc. 131, 16162–16170. https://doi.org/10.1021/ja9053459.

Clark, T., Chandrasekhar, J., Spitznagel, G.W., Schleyer, P.V.R., 1983. Efficient diffuse function-augmented basis sets for anion calculations. III. The 3-21+G basis set for first-row elements, Li–F. J. Comput. Chem. 4, 294–301. https://doi.org/10.1002/jcc.540040303.

Daru, J., Forbert, H., Behler, J., Marx, D., 2022. Coupled cluster molecular dynamics of condensed phase systems enabled by machine learning potentials: liquid water benchmark. Phys. Rev. Lett. 129, 226001 https://doi.org/10.1103/PhysRevLett.129.226001.

Dickson, A.G., 1990. Thermodynamics of the dissociation of boric acid in synthetic seawater from 273.15 to 318.15 K. Deep Sea Res. Part A 37, 755–766. https://doi.org/10.1016/0198-0149(90)90004-F.

Domagal-Goldman, S.D., Kubicki, J.D., 2008. Density functional theory predictions of equilibrium isotope fractionation of iron due to redox changes and organic complexation. Geochim. Cosmochim. Acta 72, 5201–5216. https://doi.org/10.1016/j.gca.2008.05.066.

Dunning, T.H., 1989. Gaussian basis sets for use in correlated molecular calculations. I. The atoms boron through neon and hydrogen. J. Chem. Phys. 90, 1007–1023. https://doi.org/10.1063/1.456153.

Farmer, J.R., Branson, O., Uchikawa, J., Penman, D.E., Honisch, B., Zeebe, R.E., 2019. Boric acid and borate incorporation in inorganic calcite inferred from B/Ca, boron isotopes and surface kinetic modeling. Geochim. Cosmochim. Acta 244, 229–247. https://doi.org/10.1016/j.gca.2018.10.008.

Frisch, M.J., Pople, J.A., Binkley, J.S., 1984. Self-consistent molecular orbital methods 25. Supplementary functions for Gaussian basis sets. J. Chem. Phys. 80, 3265–3269. https://doi.org/10.1063/1.447079.

Frisch, M.J., Trucks, G.W., Schlegel, H.B., Scuseria, G.E., Robb, M.A., Cheeseman, J.R., Montgomery Jr., J.A., Vreven, T., Kudin, K.N., Burant, J.C., Millam, J.M., Iyengar, S. S., Tomasi, J., Barone, V., Mennucci, B., Cossi, M., Scalmani, G., Rega, N., Petersson, G.A., Nakatsuji, H., Hada, M., Ehara, M., Toyota, K., Fukuda, R., Hasegawa, J., Ishida, M., Nakajima, T., Honda, Y., Kitao, O., Nakai, H., Klene, M., Li, X., Knox, J.E., Hratchian, H.P., Cross, J.B., Adamo, C., Jaramillo, J., Gomperts, R., Stratmann, R.E., Yazyev, O., Austin, A.J., Cammi, R., Pomelli, C., Ochterski, J.W., Ayala, P.Y., Morokuma, K., Voth, G.A., Salvador, P., Dannenberg, J.J., Zakrzewski, V.G., Dapprich, S., Daniels, A.D., Strain, M.C., Farkas, O., Malick, D.K., Rabuck, A.D., Raghavachari, K., Foresman, J.B., Ortiz, J.V., Cui, Q., Baboul, A.G., Clifford, S., Cioslowski, J., Stefanov, B.B., Liu, G., Liashenko, A., Piskorz, P., Komaromi, I., Martin, R.L., Fox, D.J., Keith, T., Al-Laham, M.A., Peng, C.Y., Nanayakkara, A., Challacombe, M., Gill, P.M.W., Johnson, B., Chen, W., Wong, M. W., Gonzalez, C., Pople, J.A., 2013. Gaussian 09, (Revision D.01). Gaussian, Inc., Wallingford CT.

Fujii, T., Moynier, F., Blichert-Toft, J., Albarede, F., 2014. Density functional theory estimation of isotope fractionation of Fe, Ni, Cu, and Zn among species relevant to geochemical and biological environments. Geochim. Cosmochim. Acta 140, 553–576. https://doi.org/10.1016/j.gca.2014.05.051.

Gao, C., Cao, X., Liu, Q., Yang, Y., Zhang, S., He, Y., Tang, M., Liu, Y., 2018. Theoretical calculation of equilibrium Mg isotope fractionations between minerals and aqueous solutions. Chem. Geol. 488, 62–75. https://doi.org/10.1016/j.chemgeo.2018.04.005.

Grimme, S., 2011. Density functional theory with London dispersion corrections. Wiley Interdiscip. Rev. Comput. Mol. Sci. 1, 211–228. https://doi.org/10.1002/wcms.30.

Grimme, S., 2012. Supramolecular binding thermodynamics by dispersion-corrected density functional theory. Chem. Eur. J. 18, 9955–9964. https://doi.org/10.1002/chem.201200497.

Harding, M.E., Metzroth, T., Gauss, J., Auer, A.A., 2008a. Parallel calculation of CCSD and CCSD(T) analytic first and second derivatives. J. Chem. Theory Comput. 4, 64–74. https://doi.org/10.1021/ct700152c.

Harding, M.E., Vazquez, J., Ruscic, B., Wilson, A.K., Gauss, J., Stanton, J.F., 2008b. High-accuracy extrapolated ab initio thermochemistry. III. Additional improvements and overview. J. Chem. Phys. 128 https://doi.org/10.1063/1.2835612.

Hemming, N.G., Hanson, G.N., 1992. Boron isotopic composition and concentration in modern marine carbonates. Geochim. Cosmochim. Acta 56, 537–543. https://doi.org/10.1016/0016-7037(92)90151-8.

Hemming, N.G., Reeder, R.J., Hanson, G.N., 1995. Mineral-fluid partitioning and isotopic fractionation of boron in synthetic calcium carbonate. Geochim. Cosmochim. Acta 59, 371–379. https://doi.org/10.1016/0016-7037(95)00288-b.

Henehan, M.J., Foster, G.L., Bostock, H.C., Greenop, R., Marshall, B.J., Wilson, P.A., 2016. A new boron isotope-pH calibration for *Orbulina universa*, with implications for understanding and accounting for 'vital effects'. Earth Planet. Sci. Lett. 454, 282–292. https://doi.org/10.1016/j.epsl.2016.09.024.

Henehan, M.J., Gebbinck, C.D.K., Wyman, J.V.B., Hain, M.P., Rae, J.W.B., Honisch, B., Foster, G.L., Kim, S.-T., 2022. No ion is an island: multiple ions influence boron incorporation into $CaCO_3$. Geochim. Cosmochim. Acta 318, 510–530. https://doi.org/10.1016/j.gca.2021.12.011.

Hershey, J.P., Fernandez, M., Milne, P.J., Millero, F.J., 1986. The ionization of boric acid in NaCl, Na-Ca-Cl and Na-Mg-Cl solutions at 25°C. Geochim. Cosmochim. Acta 50, 143–148. https://doi.org/10.1016/0016-7037(86)90059-1.

Hill, P.S., Schauble, E.A., Tripati, A., 2020. Theoretical constraints on the effects of added cations on clumped, oxygen, and carbon isotope signatures of dissolved inorganic carbon species and minerals. Geochim. Cosmochim. Acta 269, 496–539. https://doi.org/10.1016/j.gca.2019.10.016.

Hönisch, B., Hemming, N.G., 2005. Surface ocean pH response to variations in pCO_2 through two full glacial cycles. Earth Planet. Sci. Lett. 236, 305–314. https://doi.org/10.1016/j.epsl.2005.04.027.

Hönisch, B., Bickert, T., Hemming, N., 2008. Modern and pleistocene boron isotope composition of the benthic foraminifer *Cibicidoides wuellerstorfi*. Earth Planet. Sci. Lett. 272, 309–318. https://doi.org/10.1016/j.epsl.2008.04.047.

Hönisch, B., Eggins, S.M., Haynes, L.L., Allen, K.A., Holland, K.D., Lorbacher, K., 2019. Boron Proxies in Paleoceanography and Paleoclimatology, first ed. John Wiley & Sons, Hoboken, NJ. https://doi.org/10.1002/9781119010678.

Ingri, N., Lagerstrom, G., Frydman, M., Sillen, L.G., 1957. Equilibrium studies of polyanions. II. Polyborates in $NaClO_4$ medium. Acta Chem. Scand. 11, 1034–1058. https://doi.org/10.3891/acta.chem.scand.11-1034.

Kaczmarek, K., Nehrke, G., Misra, S., Bijma, J., Elderfield, H., 2016. Investigating the effects of growth rate and temperature on the B/Ca ratio and $\delta^{11}B$ during inorganic calcite formation. Chem. Geol. 421, 81–92. https://doi.org/10.1016/j.chemgeo.2015.12.002.

Kakihana, H., Kotaka, M., Satoh, S., Nomura, M., Okamoto, M., 1977. Fundamental studies on the ion-exchange separation of boron isotopes. Bull. Chem. Soc. Jpn. 50, 158–163. https://doi.org/10.1246/bcsj.50.158.

Kannath, S., Adamczyk, P., Ferro-Costas, D., Fernandez-Ramos, A., Major, D.T., Dybala-Defratyka, A., 2020. Role of microsolvation and quantum effects in the accurate prediction of kinetic isotope effects: the case of hydrogen atom abstraction in ethanol by atomic hydrogen in aqueous solution. J. Chem. Theory Comput. 16, 847–859. https://doi.org/10.1021/acs.jctc.9b00774.

Kendall, R.A., Dunning, T.H., Harrison, R.J., 1992. Electron affinities of the first-row atoms revisited. Systematic basis sets and wave functions. J. Chem. Phys. 96, 6796–6806. https://doi.org/10.1063/1.462569.

Klochko, K., Kaufman, A.J., Yao, W., Byrne, R.H., Tossell, J.A., 2006. Experimental measurement of boron isotope fractionation in seawater. Earth Planet. Sci. Lett. 248, 276–285. https://doi.org/10.1016/j.epsl.2006.05.034.

Kowalski, P.M., Wunder, B., Jahn, S., 2013. *Ab initio* prediction of equilibrium boron isotope fractionation between minerals and aqueous fluids at high *P* and *T*. Geochim. Cosmochim. Acta 101, 285–301. https://doi.org/10.1016/j.gca.2012.10.007.

Krishnan, R., Binkley, J.S., Seeger, R., Pople, J.A., 1980. Self-consistent molecular orbital methods. XX. A basis set for correlated wave functions. J. Chem. Phys. 72, 650–654. https://doi.org/10.1063/1.438955.

Kruse, H., Goerigk, L., Grimme, S., 2012. Why the standard B3LYP/6-31G* model chemistry should not be used in DFT calculations of molecular thermochemistry: understanding and correcting the problem. J. Organomet. Chem. 77, 10824–10834. https://doi.org/10.1021/jo302156p.

Kubicki, J.D., 2016. Molecular Modeling of Geochemical Reactions: An Introduction, first ed. John Wiley & Sons, Hoboken, NJ. https://doi.org/10.1002/9781118845226.

Lee, C.T., Yang, W.T., Parr, R.G., 1988. Development of the Colle-Salvetti correlation-energy formula into a functional of the electron-density. Phys. Rev. B 37, 785–789. https://doi.org/10.1103/PhysRevB.37.785.

Lee, K., Kim, T.-W., Byrne, R.H., Millero, F.J., Feely, R.A., Liu, Y.-M., 2010. The universal ratio of boron to chlorinity for the North Pacific and North Atlantic oceans. Geochim. Cosmochim. Acta 74, 1801–1811. https://doi.org/10.1016/j.gca.2009.12.027.

Lemarchand, D., Gaillardet, J., Lewin, E., Allegre, C.J., 2002. Boron isotope systematics in large rivers: implications for the marine boron budget and paleo-pH reconstruction over the Cenozoic. Chem. Geol. 190, 123–140. https://doi.org/10.1016/s0009-2541(02)00114-6.

Levine, I.N., 2014. Quantum Chemistry, seventh ed. Pearson, Upper Saddle River, NJ.

Li, X., Zhao, H., Tang, M., Liu, Y., 2009. Theoretical prediction for several important equilibrium Ge isotope fractionation factors and geological implications. Earth Planet. Sci. Lett. 287, 1–11. https://doi.org/10.1016/j.epsl.2009.07.027.

Li, Y.-C., Chen, H.-W., Wei, H.-Z., Jiang, S.-Y., Palmer, M.R., van de Ven, T.G.M., Hohl, S., Lu, J.-J., Ma, J., 2020. Exploration of driving mechanisms of equilibrium boron isotope fractionation in tourmaline group minerals and fluid: a density functional theory study. Chem. Geol. 536, 119466 https://doi.org/10.1016/j.chemgeo.2020.119466.

Li, Y.-C., Wei, H.-Z., Palmer, M.R., Jiang, S.-Y., Liu, X., Williams-Jones, A.E., Ma, J., Lu, J.-J., Lin, Y.-B., Dong, G., 2021. Boron coordination and B/Si ordering controls over equilibrium boron isotope fractionation among minerals, melts, and fluids. Chem. Geol. 561, 120030 https://doi.org/10.1016/j.chemgeo.2020.120030.

Li, Y.-C., Wei, H.-Z., Palmer, M.R., Ma, J., Jiang, S.-Y., Chen, Y.-X., Lu, J.-J., Liu, X., 2022. Equilibrium boron isotope fractionation during serpentinization and applications in understanding subduction zone processes. Chem. Geol. 609, 121047 https://doi.org/10.1016/j.chemgeo.2022.121047.

Liu, Q., Liu, Y., 2016. Clumped-isotope signatures at equilibrium of CH_4, NH_3, H_2O, H_2S and SO_2. Geochim. Cosmochim. Acta 175, 252–270. https://doi.org/10.1016/j.gca.2015.11.040.

Liu, Y., Tossell, J.A., 2005. Ab initio molecular orbital calculations for boron isotope fractionations on boric acids and borates. Geochim. Cosmochim. Acta 69, 3995–4006. https://doi.org/10.1016/j.gca.2005.04.009.

Liu, Q., Tossell, J.A., Liu, Y., 2010. On the proper use of the Bigeleisen-Mayer equation and corrections to it in the calculation of isotopic fractionation equilibrium constants. Geochim. Cosmochim. Acta 74, 6965–6983. https://doi.org/10.1016/j.gca.2010.09.014.

Liu, Q., Yin, X., Zhang, Y., Julien, M., Zhang, N., Gilbert, A., Yoshida, N., Liu, Y., 2021. Theoretical calculation of position-specific carbon and hydrogen isotope equilibriums in butane isomers. Chem. Geol. 561, 120031 https://doi.org/10.1016/j.chemgeo.2020.120031.

Mavromatis, V., Montouillout, V., Noireaux, J., Gaillardet, J., Schott, J., 2015. Characterization of boron incorporation and speciation in calcite and aragonite from co-precipitation experiments under controlled pH, temperature and precipitation rate. Geochim. Cosmochim. Acta 150, 299–313. https://doi.org/10.1016/j.gca.2014.10.024.

Mavromatis, V., Purgstaller, B., Louvat, P., Faure, L., Montouillout, V., Gaillardet, J., Schott, J., 2021. Boron isotope fractionation during the formation of amorphous calcium carbonates and their transformation to Mg-calcite and aragonite. Geochim. Cosmochim. Acta 315, 152–171. https://doi.org/10.1016/j.gca.2021.08.041.

McLean, A.D., Chandler, G.S., 1980. Contracted Gaussian basis sets for molecular calculations. I. Second row atoms, Z=11-18. J. Chem. Phys. 72, 5639–5648. https://doi.org/10.1063/1.438980.

Méheut, M., Lazzeri, M., Balan, E., Mauri, F., 2007. Equilibrium isotopic fractionation in the kaolinite, quartz, water system: prediction from first-principles density-functional theory. Geochim. Cosmochim. Acta 71, 3170–3181. https://doi.org/10.1016/j.gca.2007.04.012.

Møller, C., Plesset, M.S., 1934. Note on an approximation treatment for many-electron systems. Phys. Rev. 46, 618–622. https://doi.org/10.1103/PhysRev.46.618.

Nir, O., Vengosh, A., Harkness, J.S., Dwyer, G.S., Lahav, O., 2015. Direct measurement of the boron isotope fractionation factor: reducing the uncertainty in reconstructing ocean paleo-pH. Earth Planet. Sci. Lett. 414, 1–5. https://doi.org/10.1016/j.epsl.2015.01.006.

Noireaux, J., Mavromatis, V., Gaillardet, J., Schott, J., Montouillout, V., Louvat, P., Rollion-Bard, C., Neuville, D.R., 2015. Crystallographic control on the boron isotope paleo-pH proxy. Earth Planet. Sci. Lett. 430, 398–407. https://doi.org/10.1016/j.epsl.2015.07.063.

Oi, T., 2000a. Ab initio molecular orbital calculations of reduced partition function ratios of polyboric acids and polyborate anions. Z. Naturforsch. A 55, 623–628. https://doi.org/10.1515/zna-2000-6-710.

Oi, T., 2000b. Calculations of reduced partition function ratios of monomeric and dimeric boric acids and borates by the *ab initio* molecular orbital theory. J. Nucl. Sci. Technol. 37, 166–172. https://doi.org/10.1080/18811248.2000.9714880.

Oi, T., Yanase, S., 2001. Calculations of reduced partition function ratios of hydrated monoborate anion by the *ab initio* molecular orbital theory. J. Nucl. Sci. Technol. 38, 429–432. https://doi.org/10.3327/jnst.38.429.

Pagani, M., Lemarchand, D., Spivack, A., Gaillardet, J., 2005. A critical evaluation of the boron isotope-pH proxy: the accuracy of ancient ocean pH estimates. Geochim. Cosmochim. Acta 69, 953–961. https://doi.org/10.1016/j.gca.2004.07.029.

Palmer, M.R., Pearson, P.N., 2003. A 23,000-year record of surface water pH and pCO_2 in the western equatorial Pacific Ocean. Science 300, 480–482. https://doi.org/10.1126/science.1080796.

Palmer, M.R., Pearson, P.N., Cobb, S.J., 1998. Reconstructing past ocean pH-depth profiles. Science 282, 1468–1471. https://doi.org/10.1126/science.282.5393.1468.

Pearson, P.N., Palmer, M.R., 1999. Middle Eocene seawater pH and atmospheric carbon dioxide concentrations. Science 284, 1824–1826. https://doi.org/10.1126/science.284.5421.1824.

Pearson, P.N., Palmer, M.R., 2000. Atmospheric carbon dioxide concentrations over the past 60 million years. Nature 406, 695–699. https://doi.org/10.1038/35021000.

Purvis, G.D., Bartlett, R.J., 1982. A full coupled-cluster singles and doubles model: the inclusion of disconnected triples. J. Chem. Phys. 76, 1910–1918. https://doi.org/10.1063/1.443164.

Rae, J.W.B., Foster, G.L., Schmidt, D.N., Elliott, T., 2011. Boron isotopes and B/Ca in benthic foraminifera: proxies for the deep ocean carbonate system. Earth Planet. Sci. Lett. 302, 403–413. https://doi.org/10.1016/j.epsl.2010.12.034.

Richet, P., Bottinga, Y., Janoy, M., 1977. A review of hydrogen, carbon, nitrogen, oxygen, sulphur, and chlorine stable isotope fractionation among gaseous molecules. Annu. Rev. Earth Planet. Sci. 5, 65–110. https://doi.org/10.1146/annurev.ea.05.050177.000433.

Riley, K.E., Pitonak, M., Cerny, J., Hobza, P., 2010. On the structure and geometry of biomolecular binding motifs (hydrogen-bonding, stacking, X–H···π): WFT and DFT calculations. J. Chem. Theory Comput. 6, 66–80. https://doi.org/10.1021/ct900376r.

Rustad, J.R., Bylaska, E.J., 2007. Ab initio calculation of isotopic fractionation in B$(OH)_3$(aq) and B$(OH)_4^-$(aq). J. Am. Chem. Soc. 129, 2222–2223. https://doi.org/10.1021/ja0683335.

Rustad, J.R., Bylaska, E.J., Jackson, V.E., Dixon, D.A., 2010. Calculation of boron-isotope fractionation between B$(OH)_3$(aq) and B$(OH)_4^-$(aq). Geochim. Cosmochim. Acta 74, 2843–2850. https://doi.org/10.1016/j.gca.2010.02.032.

Saldi, G.D., Noireaux, J., Louvat, P., Faure, L., Balan, E., Schott, J., Gaillardet, J., 2018. Boron isotopic fractionation during adsorption by calcite - Implication for the seawater pH proxy. Geochim. Cosmochim. Acta 240, 255–273. https://doi.org/10.1016/j.gca.2018.08.025.

Sanchez-Valle, C., Reynard, B., Daniel, I., Lecuyer, C., Martinez, I., Chervin, J.C., 2005. Boron isotopic fractionation between minerals and fluids: new insights from *in situ* high pressure-high temperature vibrational spectroscopic data. Geochim. Cosmochim. Acta 69, 4301–4313. https://doi.org/10.1016/j.gca.2005.03.054.

Sanyal, A., Hemming, N.G., Hanson, G.N., Broecker, W.S., 1995. Evidence for a higher pH in the glacial ocean from boron isotopes in foraminifera. Nature 373, 234–236. https://doi.org/10.1038/373234a0.

Sanyal, A., Hemming, N.G., Broecker, W.S., Lea, D.W., Spero, H.J., Hanson, G.N., 1996. Oceanic pH control on the boron isotopic composition of foraminifera: evidence from culture experiments. Paleoceanography 11, 513–517. https://doi.org/10.1029/96pa01858.

Schauble, E.A., 2004. Applying stable isotope fractionation theory to new systems. Rev. Mineral. Geochem. 55, 65–111. https://doi.org/10.2138/gsrmg.55.1.65.

Simon, L., Lecuyer, C., Marechal, C., Coltice, N., 2006. Modelling the geochemical cycle of boron: implications for the long-term δ^{11}B evolution of seawater and oceanic crust. Chem. Geol. 225, 61–76. https://doi.org/10.1016/j.chemgeo.2005.08.011.

Spitznagel, G.W., Clark, T., von Ragué Schleyer, P., Hehre, W.J., 1987. An evaluation of the performance of diffuse function-augmented basis sets for second row elements, Na-Cl. J. Comput. Chem. 8, 1109–1116. https://doi.org/10.1002/jcc.540080807.

Spivack, A.J., You, C.F., Smith, H.J., 1993. Foraminiferal boron isotope ratios as a proxy for surface ocean pH over the past 21 Myr. Nature 363, 149–151. https://doi.org/10.1038/363149a0.

Urey, H.C., 1947. The thermodynamic properties of isotopic substances. J. Chem. Soc. 562–581. https://doi.org/10.1039/jr9470000562.

Vengosh, A., Kolodny, Y., Starinsky, A., Chivas, A.R., McCulloch, M.T., 1991. Coprecipitation and isotopic fractionation of boron in modern biogenic carbonates. Geochim. Cosmochim. Acta 55, 2901–2910. https://doi.org/10.1016/0016-7037(91)90455-e.

Wang, W., Huang, S., Huang, F., Zhao, X., Wu, Z., 2020. Equilibrium inter-mineral titanium isotope fractionation: implication for high-temperature titanium isotope geochemistry. Geochim. Cosmochim. Acta 269, 540–553. https://doi.org/10.1016/j.gca.2019.11.008.

Woon, D.E., Dunning, T.H., 1993. Gaussian basis sets for use in correlated molecular calculations. III. The atoms aluminum through argon. J. Chem. Phys. 98, 1358–1371. https://doi.org/10.1063/1.464303.

Xu, X., Goddard, W.A., 2004. The X3LYP extended density functional for accurate descriptions of nonbond interactions, spin states, and thermochemical properties. Proc. Natl. Acad. Sci. U. S. A. 101, 2673–2677. https://doi.org/10.1073/pnas.0308730100.

Zeebe, R.E., 2005. Stable boron isotope fractionation between dissolved $B(OH)_3$ and B$(OH)_4^-$. Geochim. Cosmochim. Acta 69, 2753–2766. https://doi.org/10.1016/j.gca.2004.12.011.

Zeebe, R.E., Rae, J.W.B., 2020. Equilibria, kinetics, and boron isotope partitioning in the aqueous boric acid-hydrofluoric acid system. Chem. Geol. 550, 119693 https://doi.org/10.1016/j.chemgeo.2020.119693.

Zhang, Y., Liu, Y., 2018. The theory of equilibrium isotope fractionations for gaseous molecules under super-cold conditions. Geochim. Cosmochim. Acta 238, 123–149. https://doi.org/10.1016/j.gca.2018.07.001.